Orientation Effects on Critical Heat Flux From Discrete, In-Line Heat Sources in a Flow Channel

C. O. Gersey
Graduate Student.

I. Mudawar
Professor and Director.

Boiling and Two-Phase Flow Laboratory,
School of Mechanical Engineering,
Purdue University,
West Lafayette, IN 47907

The effects of flow orientation on critical heat flux (CHF) were investigated on a series of nine in-line simulated microelectronic chips in Fluorinert FC-72. The chips were subjected to coolant in upflow, downflow, or horizontal flow with the chips on the top or bottom walls of the channel with respect to gravity. Changes in angle of orientation affected CHF for velocities below 200 cm/s, with some chips reaching CHF at heat fluxes below the pool boiling and flooding-induced CHF values. Increased subcooling was found to dampen this adverse effect of orientation slightly. Critical heat flux was overwhelmingly caused by localized dryout of the chip surface. However, during the low velocity downflow tests, low CHF values were measured because of liquid blockage by vapor counterflow and vapor stagnation in the channel. At the horizontal orientation with downward-facing chips, vapor/liquid stratification also yielded low CHF values. Previously derived correlations for water and long, continuous heaters had limited success in predicting CHF for the present discontinuous heater configuration. Because orientation has a profound effect on the hydrodynamics of two-phase flow and, consequently, on CHF for small inlet velocities, downflow angles should be avoided, or when other constraints force the usage of downflow angles, the inlet liquid velocity should be sufficiently large.

Introduction

With the continuing trend of miniaturization of electronic components in chips, power dissipation from the chip is expected to continue to increase during the present and next decades. As a result, a need has arisen in the electrical packaging industry for new cooling schemes capable of dissipating heat from densely packaged, high-heat-flux systems. Direct immersion cooling in a dielectric fluid with nucleate boiling on the chip surface holds the promise of dissipating high heat fluxes while maintaining the chip at an acceptable operating temperature. However, as in any boiling system, the nucleate boiling regime is limited by the critical heat flux (CHF). Exceeding this heat flux limit causes a vapor blanket to form on the boiling surface, severely decreasing the heat transfer coefficient, which, in turn, causes the surface temperature to increase greatly and the component to fail. Predicting CHF has, therefore, become of paramount importance to the electronic packaging industry before direct immersion cooling with phase change can be utilized.

The nuclear industry has extensively studied CHF, but nuclear simulation systems do not accurately represent electrical components, such as circuit boards, with many small independent heat sources. This forced researchers in recent years to undertake new efforts specifically tailored to the needs of the electronic industry. Attention in these efforts has been focused on determining CHF from a small isolated heat source in pool (Nakayama et al., 1984; Park and Bergles, 1988; Mudawar and Anderson, 1989a, b; Park et al., 1990) and forced-convection boiling (Lee and Simon, 1989; Maddox and Mudawar, 1989; Mudawar and Maddox, 1989, 1990; Samant and Simon, 1989). Mudawar and Maddox (1989) investigated CHF on a single flush-mounted, 12.7 mm × 12.7 mm chip in vertical upflow of FC-72. Critical heat flux was observed to be a result of localized vapor blanketing on the chip surface. They constructed a semi-empirical CHF model from their data according to the following equation:

$$q_m^{**} = \frac{\dfrac{q_m''}{\rho_g U h_{fg}}}{\left(\dfrac{\rho_f}{\rho_g}\right)^{15/23}\left(\dfrac{L}{D_h}\right)^{1/23}\left(1+\dfrac{c_{pf}\Delta T_{sub}}{h_{fg}}\right)^{7/23}\left(1+0.021\,\dfrac{\rho_f}{\rho_g}\,\dfrac{c_{pf}\Delta T_{sub}}{h_{fg}}\right)^{16/23}} = 0.161\,(\mathrm{We})^{-8/23}. \quad (1)$$

Mudawar and Maddox also observed a change in the slope of their CHF data marking transition between low- and high-velocity CHF regimes. Low-velocity CHF was initiated by the propagation of a fairly continuous vapor blanket, which originated from the downstream edge of the chip. High-velocity CHF was characterized by the merging of smaller patches of vapor on the chip surface.

Only a few studies are available in the literature on CHF from simulated multichip arrays in forced-convection boiling (McGillis et al., 1991; Willingham et al., 1991; Willingham and Mudawar, 1992a, b). McGillis et al. (1991) found that Eq. (1) accurately predicted CHF for their flush-mounted, ten-element array in vertical upflow of R-113. Typically, the last chip in the array attained CHF first, and McGillis et al. used a calculated local subcooling for that chip in utilizing Eq. (1). Invariably, the heat sources in previous studies have been oriented either vertically or horizontally. So far, little attention has been focused on the detailed effects of orientation on forced-convection CHF from simulated microelectronic chips.

Contributed by the Heat Transfer Division for publication in the JOURNAL OF HEAT TRANSFER. Manuscript received by the Heat Transfer Division December 1992; revision received March 1993. Keywords: Boiling, Phase-Change Phenomena, Thermal Packaging. Associate Technical Editor: T. W. Simon.

Many researchers have tested the effect of surface orientation in pool boiling (Class et al., 1960; Githinji and Sabersky, 1963; Marcus and Dropkin, 1963; Chen, 1978; Nishikawa et al., 1983; Kumar et al., 1990) and forced-convection boiling (Simoneau and Simon, 1966; Bartolini et al., 1983; Mishima and Nishihara, 1985; Mishima et al., 1985; Bibeau and Salcudean, 1990) for various experimental configurations unrelated to electronic cooling; however, a full accounting of the orientation effect throughout a 360 deg circle on CHF with an array of discrete heat sources during flow boiling has never been made. This has important implications for design engineers since a thermal analysis is typically performed after the electronic package has been designed. Understanding the g-field effect on boiling performance will aid, perhaps, in formulating constraints on the chip orientation at the onset of the design process as well as providing some guidance in predicting the g-field effect in nonterrestrial environments such as microgravity and vehicular acceleration induced. Beside electronics, heat removal from small sources with varying orientations is also encountered in other applications such as laser devices, x-ray machines, and power supplies.

In the pool boiling studies reviewed, an increase in the nucleate boiling heat transfer coefficient was observed as the surface was rotated away from both horizontal positions (Class et al., 1960; Githinji and Sabersky, 1963; Marcus and Dropkin, 1963; Chen, 1978; Kumar et al., 1990). However, Nishikawa et al. (1983) observed little effect of orientation at high heat fluxes. Critical heat flux decreased severely when the heated surface was oriented in the horizontal, downward-facing position due to vapor accumulation, which kept liquid from reaching the heated surface.

Flow Boiling Orientation Studies

Because of the large density difference between the vapor and liquid phases, two-phase instabilities can occur during low-velocity forced-convection boiling involving downflow. During stable downflow, the vapor bubbles are entrained in the liquid flow forming a two-phase mixture. One type of unstable downflow is characterized by the vapor and the liquid moving in opposite directions because the buoyancy force acting on the vapor is greater than the drag force exerted by the liquid. Changes in vapor motion, from countercurrent at low liquid velocities to cocurrent at high liquid velocities, were observed during the forced-convection boiling of nitrogen in a vertical channel subjected to downflow (Simoneau and Simon, 1966). The liquid nitrogen velocity was varied between 25.9 and 106.7 cm/s for both upflow and downflow, and CHF was observed to be lower for downflow as compared to upflow tests at the same liquid velocity. The difference between upflow and downflow CHF decreased with increasing liquid velocity due to the diminishing effect of buoyancy. In a review article, Gambill (1968) noted that, in some of his previous work with boiling in a vertical channel at very low velocities, the CHF values for downflow were several times smaller than for upflow. The lowest downflow CHF value was measured when the liquid velocity was equal to the bubble rise velocity in the channel.

Mishima et al. (1985) studied the effect of upflow and downflow on CHF in a 6-mm tube in a soft flow loop design, where the flow rate was controlled through a bypass line and a throttle valve upstream of the tube. Downflow CHF values were lower than their upflow counterparts. In addition, the flow rate in downflow tests vacillated around the mean value at a high frequency as the heat flux was increased. A few minutes before CHF, the mean flow rate decreased purportedly as a result of the compressibility of the vapor in the flow loop. No adjustment was made to the flow rate, and CHF ensued. In order to investigate the effects of a compressible volume on flow rate and hence, CHF, a plenum with a volume of 1077 cm^3 was added upstream of the tube. The stagnation of vapor in the tube was found to contribute to a premature CHF in downflow tests. Critical heat flux for all of the downflow conditions tended toward the flooding-induced CHF value as flow rate was decreased to zero.

Mishima and Nishihara (1985) studied similar low-velocity effects of upflow and downflow on CHF in a 2.4 mm × 40 mm rectangular channel. The channel was heated on either one or two of the 40-mm sides, and flow throttling was performed upstream of the test section (soft system). Several flow regimes were observed for low inlet liquid velocities. At extremely small flow rates, CHF was triggered by flooding in downflow. Similarly, for upflow conditions, flooding was observed to cause CHF at small flow rates as the vapor kept liquid from flowing backward into the test section and rewetting the heated surface. Annular flow appeared in the downstream portion of the channel as the flow rate was in-

Nomenclature

A_{he} = heated area (900 mm^2 for the present study)
A_x = channel flow area
c_{pf} = specific heat of liquid
D_h = channel hydraulic diameter = $4A_x/P_{wet}$
D_{he} = equivalent heated channel diameter = $4A_x/P_{he}$
g = gravitational acceleration
G = mass velocity
G^* = nondimensional mass velocity = $G/[\rho_g g(\rho_f - \rho_g)\lambda]^{0.5}$
Δh_i = subcooled liquid enthalpy at inlet = $c_{pf}\Delta T_{sub}$
h_{fg} = latent heat of vaporization
k_f = thermal conductivity of liquid
L = chip length in flow direction (10 mm)
L_{he} = heated length (90 mm for the present study)
P = pressure
P_{he} = heated perimeter of channel (10 mm for the present study)
P_{wet} = wetted perimeter of channel
q'' = wall heat flux
q^* = nondimensional heat flux = $q''/[h_{fg}(\rho_g g(\rho_f - \rho_g)\lambda)^{0.5}]$
q''_m = critical heat flux
q^{**}_m = nondimensional critical heat flux defined in Eq. (1)
t = time
T = temperature
ΔT_{sub} = inlet subcooling = $T_{sat} - T_{f,in}$
U = mean inlet liquid velocity
We = Weber number = $(\rho_f U^2 L)/\sigma$
x_e = thermodynamic equilibrium quality
λ = length scale of the Taylor instability = $(\sigma/g(\rho_f - \rho_g))^{0.5}$
ρ = density
σ = surface tension
θ = orientation angle measured from the vertical position

Subscripts

ca = churn turbulent to annular flow transition
f = liquid
F = flooding-induced CHF correlation
g = vapor
H = H-regime CHF correlation, Table 2
HP = HP-regime CHF correlation, Table 2
in = inlet to multichip module
K = Katto and Kurata small L_{he}/D_{he} CHF correlation, Table 2
MM = Mudawar and Maddox CHF correlation, Table 2
pb = pool boiling CHF correlation, Table 2
sat = saturated
$x0$ = corresponding to $x_e = 0$
$x1$ = corresponding to $x_e = 1$

creased for upflow conditions; CHF for these conditions increased with increasing flow rate. As the flow rate was increased for downflow, the bubbles became motionless in the channel as the drag force of the incoming liquid equaled the buoyancy force acting on the bubble; as a result, CHF occurred at an even lower heat flux than for flooding. Bubbles became entrained in the liquid flow with a further increase in flow rate above the stagnation value, and CHF increased. For highly subcooled flow and relatively high flow rates, CHF was observed to occur at the transition between the churn-turbulent and annular flow regimes for upflow and at a liquid thermodynamic quality of zero for downflow. However, because of flooding and bubble stagnation, CHF in a forced-convection boiling system subjected to a small downflow liquid velocity may be considerably lower than CHF in pool boiling.

It is apparent from the findings of Mudawar and Maddox (1989), Mishima et al. (1985), and Mishima and Nishihara (1985) that CHF may result from a number of possible flow and heat transfer induced phenomena. The focus of this paper is to examine these various forms of CHF and assess the applicability of existing CHF correlations to forced-convection boiling from an array of discrete heat sources at different surface orientations.

The flush-mounted multichip module design was chosen to simulate a series of computer chips because this basic design allowed insight into the fundamental understanding of orientation effects without complications arising from variable chip designs. Currently the literature contains orientation studies on systems with heated walls and not on small discrete heat sources typical of a computer. The present study serves to enlighten design engineers to orientation effects in two-phase cooling while serving as a basis for future comparison with studies performed on actual circuit boards with complicated geometries.

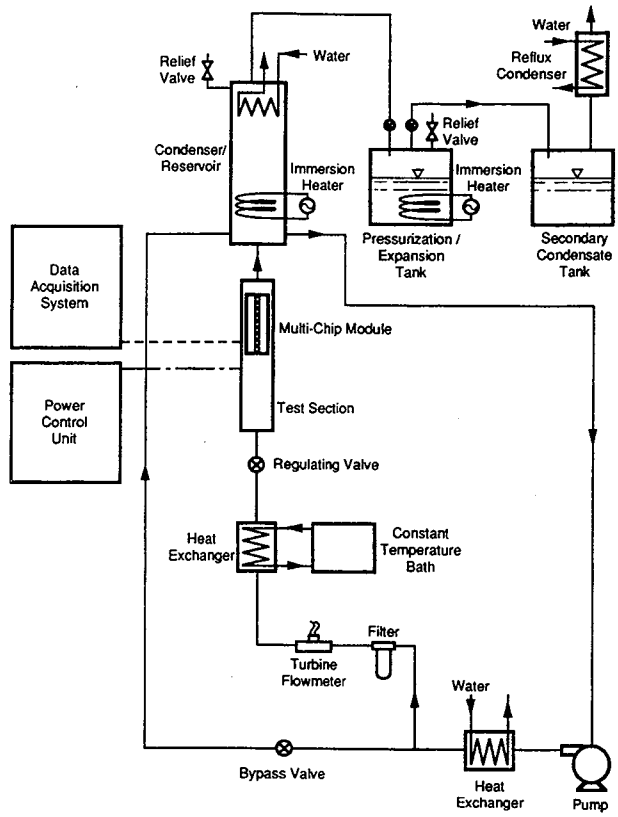

Fig. 1 Flow loop

Experimental Apparatus

A two-phase flow loop, shown in Fig. 1, circulated and conditioned the FC-72 fluid to the desired inlet flow velocity, temperature, and pressure. Liquid was forced through the loop by a magnetically coupled, centrifugal pump. Only a fraction of the total flow entered the test section while the rest was routed around the test section through a bypass line. Flow rate in the test section was controlled by two regulating valves and measured by one of two turbine flowmeters. Fluid temperature at the inlet to the test section was maintained by two heat exchangers. After leaving the test section, the fluid entered a condenser/reservoir where it recombined with the fluid from the bypass line. FC-72, a product of 3M Company, is derived from hydrocarbon compounds by replacing all of the hydrogen atoms bonded to carbon atoms with fluorine atoms.

The test section, Fig. 2(*a*), was comprised of the flow channel, upstream and downstream reservoirs, and multichip module. A support frame allowed the entire test section to rotate in 45-deg increments. A honeycomb section in the upstream reservoir served to straighten the flow and break up any large turbulent eddies. The upstream reservoir converged the flow to the channel dimensions of 20.0 mm wide by 5.0 mm high, and the flow was hydrodynamically developed in the remainder of the channel before it reached the chips. The most upstream edge of the first chip was 524.5 mm from the upstream reservoir. The rest of the chips were positioned linearly downstream of the first chip at a pitch of 20.0 mm. As shown in Fig. 2(*a*), the most upstream chip was referred to as Chip 1, and the remaining chips were sequentially assigned numbers up to nine. Three exit ports were machined in the downstream reservoir of the test section to eliminate the possibility of vapor trapping at different test section orientations.

A Lexan window housed the pressure taps, and served as the top cover for the channel. The multichip module with the flush-mounted chips formed the opposite wall at the location of the chips. Absolute and differential pressure measurements were made at Chip 1 and between Chips 1 and 9, respectively. In order to prevent air leaks into the system, the pressure in the condenser/reservoir was kept slightly above atmospheric. This caused the pressure at Chip 1 to be 1.36 bar (20 psia), which was maintained for all of the experiments. Also shown in Fig. 1, are a submerged water-cooled condenser and two immersion heaters located in the condenser/reservoir, which, along with a pressurization/expansion tank, maintained a stable system pressure within $\pm$ 0.0103 bar ($\pm$0.15 psi). The pressure at Chip 1, 1.36 bar, was taken to be the reference saturation pressure for the entire multichip array, and inlet subcooling was then calculated as the difference between the corresponding saturation temperature and the fluid temperature in the upstream reservoir. The fluid temperature in the upstream reservoir was within 0.2°C from the temperature measured by a thermocouple probe introduced into the flow at Chip 1 through the Lexan window, so liquid temperature in all the experiments was measured only in the upstream reservoir to avoid disrupting the flow in the channel by the thermocouple probe.

Figure 3 illustrates the nomenclature used to define the angle of orientation. The 0-deg reference was taken to be the vertical position with the fluid flow opposing gravity (upflow). The angle increases from 0 as the test section rotates in both directions with positive angles referring to orientations in which the chip surfaces were upward facing with respect to gravity, and negative angles to orientations in which the chip surfaces were downward facing.

The simulated chips, Fig. 2(*b*), were machined from oxygen-free copper such that the chip surface in contact with the fluid measured 10.0 mm $\times$ 10.0 mm. A thick-film resistor was silver soldered to the underside of the copper block. Three chromel-

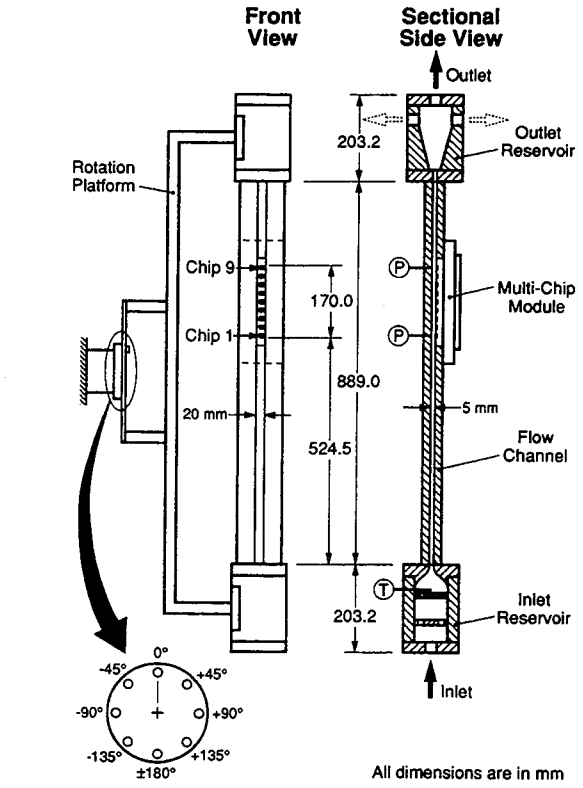

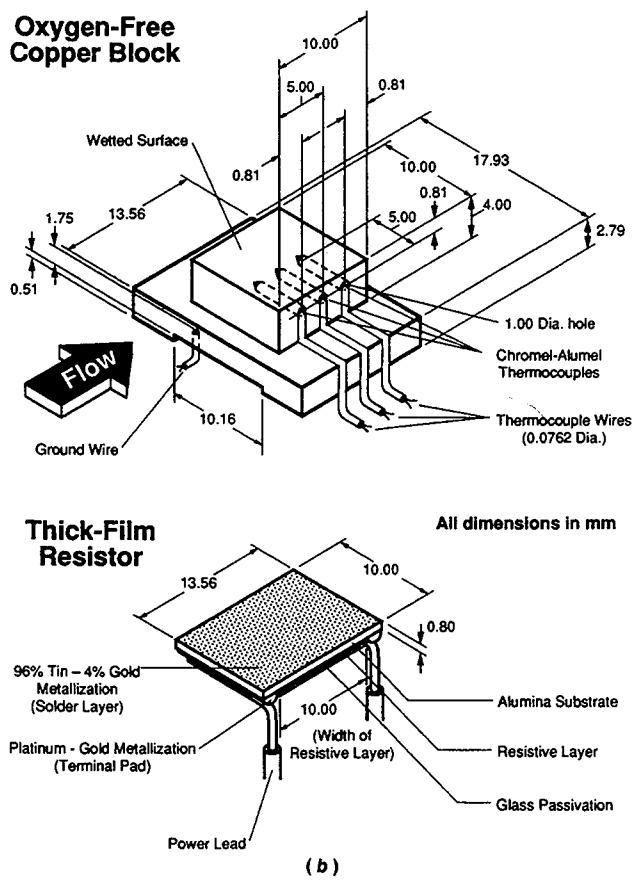

Fig. 2 Schematic of (*a*) test section and (*b*) simulated microelectronic chip

alumel thermocouples were inserted below the boiling surface and aligned along the chip centerline. One-dimensional heat conduction was used to calculate the surface temperature above

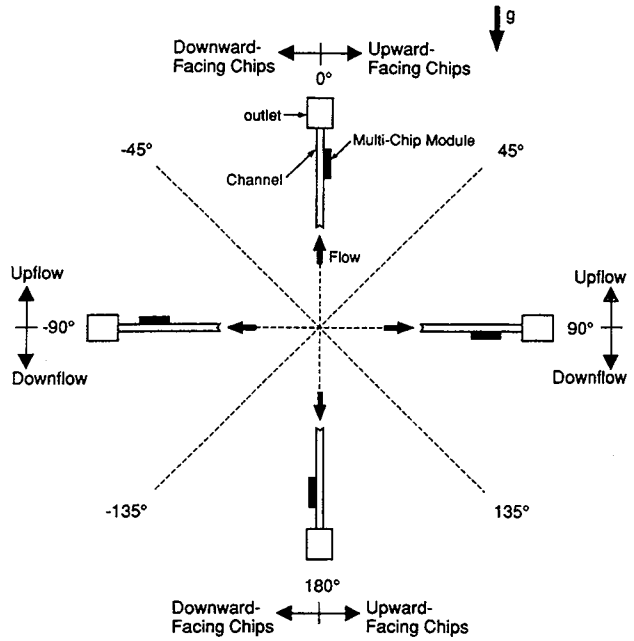

Fig. 3 Nomenclature for the angle of orientation

each of the three thermocouples, and a weighted average of the three surface temperatures set the mean surface temperature. The uniformity of the surface heat flux can be inferred from the closeness of the three thermocouple readings to each other except immediately preceding both the incipience of nucleate boiling and CHF where the streamwise temperature gradient across the chip was at most 1°C. A parallel electrical circuit powered the nine thick-film resistors. Nine variable resistors were installed in series with each chip and adjusted so that each thick-film resistor dissipated the same power. With the voltage across each chip being the same, one voltage transducer and nine current transducers were used to calculate the power dissipation of each chip. In order to save the thick-film resistor from burnout, the data acquisition system independently shut off the electric power input to each chip once that chip had reached CHF.

The chip surfaces were blasted with a water–particulate slurry prior to each set of experiments. The particles had an average size of 10 μm and served to create a uniform surface texture on each chip. Each time the system was started, the flow loop was deaerated by heating the fluid to its saturation temperature and allowing the vapor and air mixture to escape into the condensate tank. From the condensate tank, the vapor/air mixture entered a condenser where the vapor condensed and returned to the tank while the air escaped to the atmosphere. After deaerating for twenty minutes, the valve between the pressurization/expansion and condensate tanks was closed. Utilizing a gas chromatographic technique, Danielson et al. (1987) found that the air concentration in similar Fluorinerts was less than 1 percent by volume after only three minutes of deaeration; hence, a deaeration time of twenty minutes was chosen to deaerate the larger system sufficiently. The procedure for obtaining the data consisted of rotating the test section to the desired angle and then taking all of the data over the desired velocity and subcooling ranges. The standard daily procedure was to start with a particular subcooling and vary the velocity. Repeatability data were taken daily and checked with previous data obtained at the prescribed angle. Most of the CHF data were repeatable to ± 2.5 percent. The downflow orientations with low velocities had more scatter; however, almost all of those tests were repeatable within ±5 percent. On occasion, the channel was oriented to a previously tested angle, and repeatability checks were also performed.

Table 1 Experimental uncertainty

Experimental Reading	Maximum Experimental Uncertainty ± % of value	Experimental Uncertainty Estimation
Thermocouple	3.64	Manufacturer, Calibration
Heat Flux (voltage and current transducers)	7.5 at 5.7 W/cm^2 3.3 at 30.0 W/cm^2 1.6 at 120. W/cm^2	Calibration
Flowmeter ($U \leq 75$ cm/s)	1.0	Manufacturer
Flowmeter ($U > 75$ cm/s)	2.68	Manufacturer
Absolute Pressure	0.75	Manufacturer
Differential Pressure	8.0	Manufacturer

A data point was taken after the entire system attained steady state. Most of the time, steady state was reached when all the chip temperatures and the upstream reservoir temperature had 20 consecutive readings with a standard deviation of less than 0.1°C. At some orientations, the chip temperature during low-velocity test oscillated by as much as ±1.5°C at heat fluxes close to CHF. In these instances, steady state was assumed to occur when the oscillations became steady and repeatable over several sets of temperature readings. Near CHF, the heat flux increments were decreased to 0.5 W/cm^2 to ensure that CHF was not reached prematurely. A large and rapid increase in the chip temperature always signaled the attainment of CHF. Critical heat flux was approximated as the last stable heat flux plus one half of the last power increment.

The maximum percent uncertainty associated with each experimental reading is given in Table 1. Propagation of error (Moffat, 1988) was utilized, where appropriate, in calculating these uncertainties. The one-dimensional heat conduction adjustment introduced an additional uncertainty of at most ± 0.1°C in the chip surface temperature. Heat losses from the chips were minimized by constructing the multichip module from G-7 fiberglass. A two-dimensional numerical analysis was performed on a cross-sectional slice of the multichip module in order to estimate the heat losses from the chips. Heat transfer coefficients for the free convection between the backside of the multichip module and ambient air and the single-phase forced convection between the G-7 substrate and the fluid were calculated from classical correlations. The boiling heat transfer coefficient from the chip surface was adjusted until the predicted temperature at the location of the chip thermocouple agreed with the measured value. The estimated value was always within 3 percent of that based on zero heat loss. The analysis was extended to three dimensions by accounting for losses through the other transverse sides of the chip. This extension assumed that the heat flux from the chip to the substrate was the same in the three dimensions as it was in the two-dimensional model. Contact resistance between the chip and substrate was assumed to be negligible. The largest heat loss for all experiments was calculated to be 3 percent. In light of the small heat losses, the chip heat flux was taken to be the power dissipated by the thick-film resistor.

Results and Discussion

Critical heat flux data were taken using FC-72 for each of the nine chips at eight orientations spaced 45 deg apart. At each orientation, the flow velocity was varied between 13 and 400 cm/s for subcoolings of 3, 14, 25, and 36°C and an inlet pressure of 1.36 bar. Data for the 0-deg orientation were examined by Willingham and Mudawar (1992b), and the effects of orientation on the single-phase and nucleate boiling regimes were reported earlier by Gersey and Mudawar (1992).

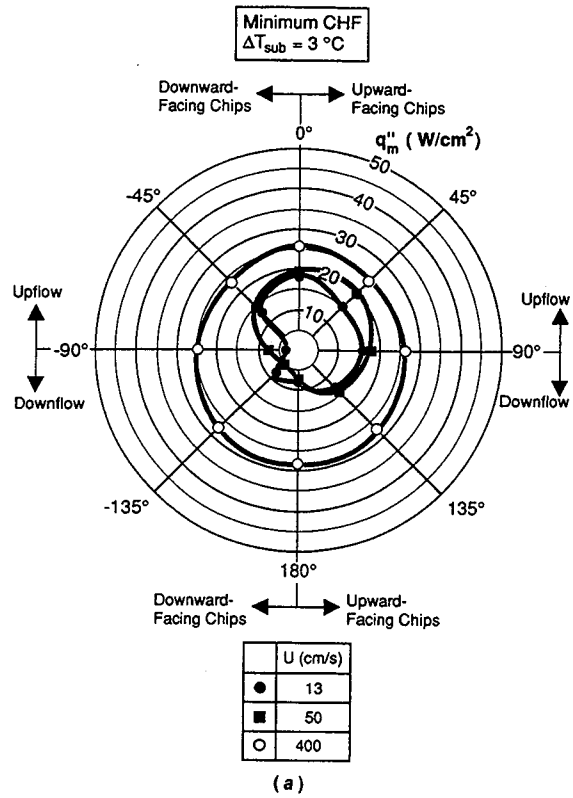

Fig. 4 Polar representation of the velocity effect on the minimum critical heat flux in the multichip array at an inlet subcooling of (*a*) 3°C and (*b*) 36°C

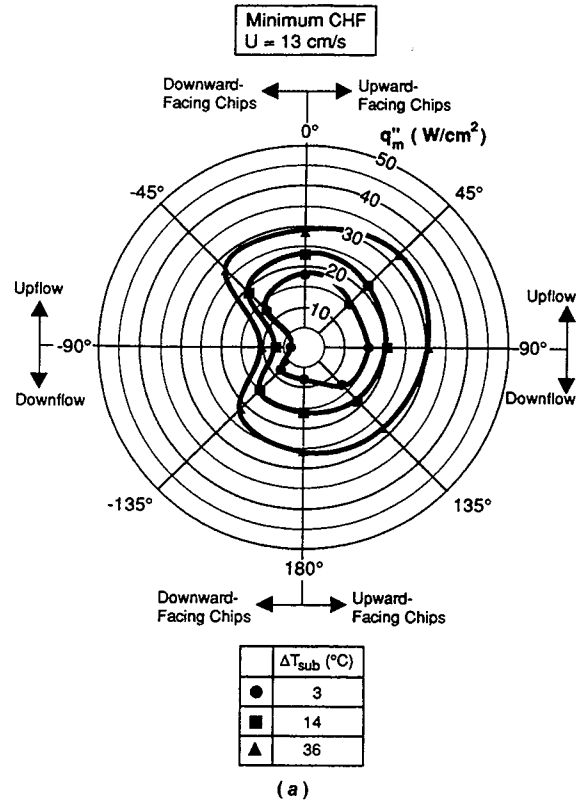

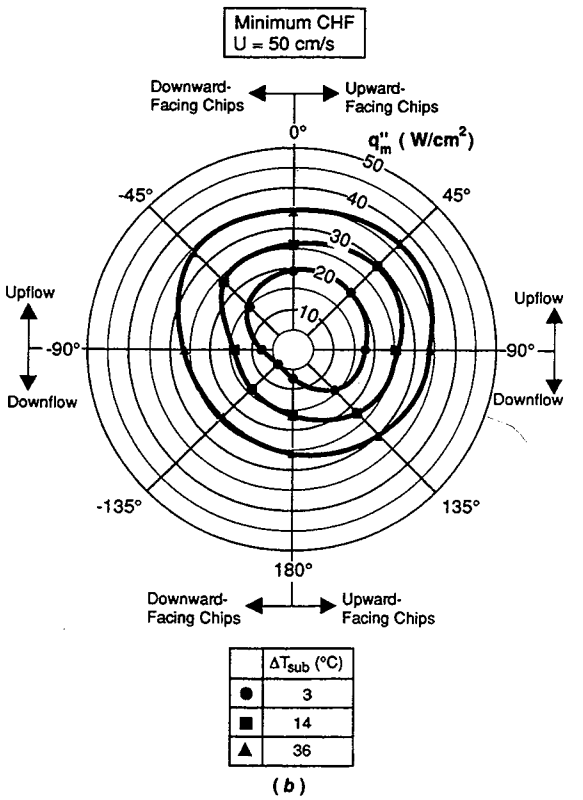

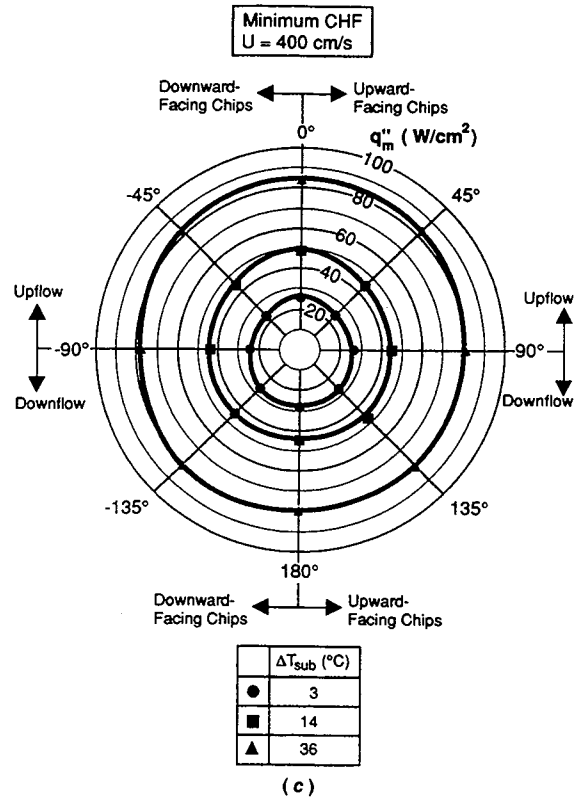

Fig. 5 Polar representation of the subcooling effect on the minimum critical heat flux in the multichip array at an inlet velocity of (*a*) 13 cm/s, (*b*) 50 cm/s, and (*c*) 400 cm/s

Minimum Critical Heat Flux in the Multichip Array. Prior to CHF, the liquid and vapor flow characteristics in the channel and at the chip surface were observed to fall into four categories:

1 Local dryout of the chip surface
2 Stratification of liquid and vapor
3 Vapor stagnation in the channel
4 Vapor counterflow causing liquid blockage

Localized dryout, similar to that observed by Mudawar and Maddox (1989), was responsible for an overwhelming majority of the CHF's. But during the downflow tests in the low velocity region, CHF was dependent on the relative motion of the liquid and vapor. Figures 4(*a*) and 4(*b*) show the effect of velocity on the minimum CHF in the multichip module in polar form. The minimum CHF is the heat flux at which the first chip, not necessarily Chip 1, reached CHF during each test. Since damage will occur to an electronic system once any chip reaches CHF, the minimum CHF value can be thought of as the prevailing design constraint. Except for the low-velocity tests at the downflow orientations, CHF generally increased with increasing inlet liquid velocity. At $\theta = -90$ deg, the vapor was observed to separate from the liquid in the channel and form stratified flow at $U = 13$ cm/s. The absence of liquid contact on the downstream chips promoted an extremely low CHF. Increases in liquid velocity were observed to retard the phase stratification and increase CHF. When the test section was oriented at $\theta = -135$ deg, CHF was actually higher for the near-saturated test at $U = 13$ cm/s as compared to $U = 25$ and 50 cm/s because the vapor moved counter to the liquid flow producing a large degree of mixing around the chips. At 25 cm/s, the vapor stagnated in the channel restricting liquid from contacting the chip surface causing a low CHF. By $U = 50$ cm/s, the drag force of the liquid became large enough to entrain the vapor; critical heat flux then increased with increasing velocity.

Figure 4(*a*) shows at $\theta = 180$ deg, the CHF values are approximately equal at both $U = 13$ cm/s (vapor counterflow) and 50 cm/s (cocurrent flow); however, the CHF values were much lower at the intermediate velocity of $U = 25$ cm/s as a result of vapor stagnation. Because the chips were upward facing at the 135-deg orientation, the stagnant bubbles pre-

dominantly rested on the Lexan window. Large-scale flow rate fluctuations prior to CHF, like those observed by Mishima et al. (1985), were never observed during the present experiments. As shown in Fig. 4(*a*), the effect of orientation on CHF became negligible for near-saturated flow for velocities greater than 200 cm/s as localized dryout was responsible for CHF for all orientations.

Lowering the inlet liquid temperature slightly dampened the effect of orientation on CHF as shown in Fig. 4(*b*). The CHF values were, again, noticeably lower at $\theta = 180$, -135, and -90 deg compared to the 0-deg reference for the low velocities. Typically, in highly subcooled flow, vapor completely condensed downstream of the chip, except at $\theta = -90$ deg, where the vapor and liquid separated, and thus, vapor could not readily condense. Vapor stagnation was still observed to lower CHF at $U = 25$ cm/s for these highly subcooled tests.

The effect of subcooling on the minimum CHF is highlighted in Figs. 5(*a*), 5(*b*), and 5(*c*) for inlet velocities of 13, 50, and 400 cm/s, respectively. The dampening of the effect of orientation on CHF with subcooled flow for downward-facing chips in downflow, $\theta = -90$, -135, and 180 deg, is further evident by comparing the angular dependence of the near-saturated and highly subcooled data in Figs. 5(*a*) and (*b*). As mentioned earlier, increasing the subcooling caused the disparity between the CHF values for upflow and downflow angles to lessen. Unlike the $U = 13$ cm/s test at $\theta = -90$ deg, vapor and liquid did not separate and remained in contact with all of the chip surfaces at $U = 50$ cm/s, and consequently, the CHF values do not show as sharp of a decrease at $\theta = -90$ deg in Fig. 5(*b*) as they do in Fig. 5(*a*). Figure 5(*c*) shows that the effect of orientation is negligible for $U = 400$ cm/s at all subcoolings. Visually, no angular dependence in boiling characteristics was observed in the channel for velocities greater than 200 cm/s with near-saturated conditions and greater than 150 cm/s with highly subcooled flow.

Critical Heat Flux Results for Individual Chips. As CHF was attained on a chip, the electrical power to that chip was shut off, and the experiment continued until all of the chips reached CHF. This facilitated the recording of the minimum CHF for the multichip array as well as a CHF value for each individual chip. Although the fluid conditions change in the channel as heaters are turned off, the continuation of the tests until all chips reached CHF elucidate important trends concerning the order of CHF occurrence in a multiheat source module. The CHF values for Chips 1, 4, and 9 are plotted versus inlet velocity for near-saturated flow in Figs. 6(*a*), 6(*b*), and 6(*c*), respectively. The relatively tight grouping of the data for the upflow angles and the spread in the data from the downflow angles shown in the earlier polar plots are evident in all three figures. The CHF values from the downflow, downward-facing chips are also clearly shown to be lower than the rest of the orientations. The lowest CHF values for Chip 1 and 4 occurred at $\theta = -135$ deg and $U = 25$ cm/s as a result of vapor bubble stagnation over the chip surface. In contrast, the lowest CHF value for Chip 9 occurred at $\theta = -90$ deg and $U = 13$ cm/s because of the local dryout caused by the vapor/liquid stratification.

In the midvelocity range, $U = 125$ to 200 cm/s, Chip 1 experienced a decrease in CHF for the near-saturated tests at all orientations. This decrease was repeatable, and since the other chips did not experience similar decreases, the anomalous behavior of Chip 1 in this velocity range was not investigated further. The transition between the low- and high-velocity CHF regimes, observed by Mudawar and Maddox (1989), are denoted on Figs. 6(*a*), 6(*b*), and 6(*c*). In the high-velocity CHF regime, the CHF data from all of the chips in the present study showed less scatter as the effect of orientation became negligible.

Figures 7(*a*), 7(*b*), and 7(*c*) show the CHF values for Chips

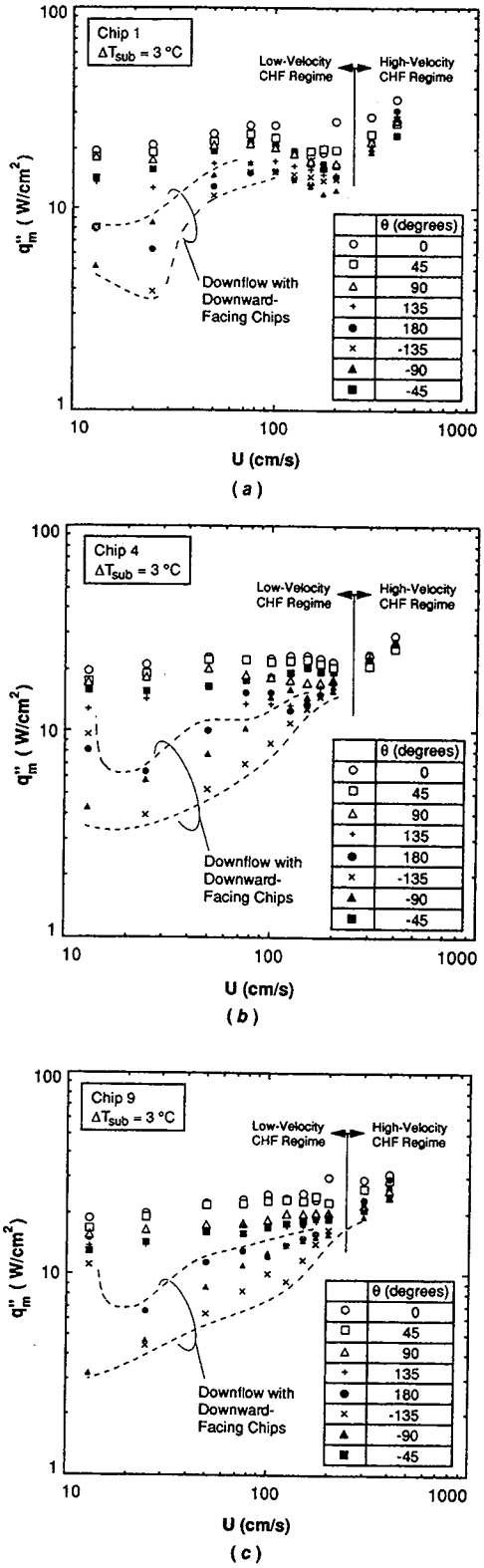

Fig. 6 Velocity effect on the critical heat flux for (*a*) Chip 1, (*b*) Chip 4, and (*c*) Chip 9 for an inlet subcooling of 3°C

1, 4, and 9, respectively, at an inlet subcooling of 25°C. As discussed earlier, increased subcooling dampened the effect of orientation. A substantial decrease in CHF for downward-facing chips with downflow is still evident from the data as well as the relative closeness of the upflow data. The effect of orientation also appears to become negligible at the transition between the low- and high-velocity CHF regimes that occurs

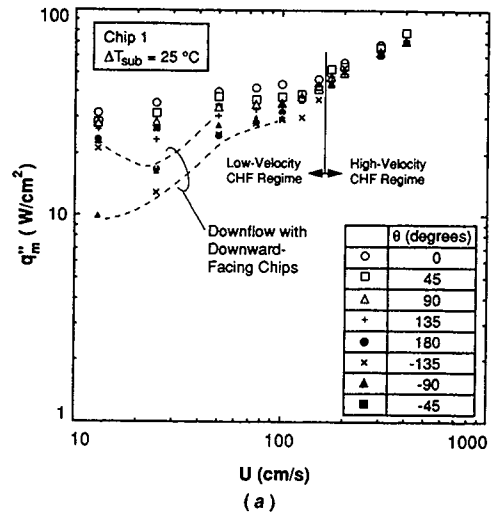

(a)

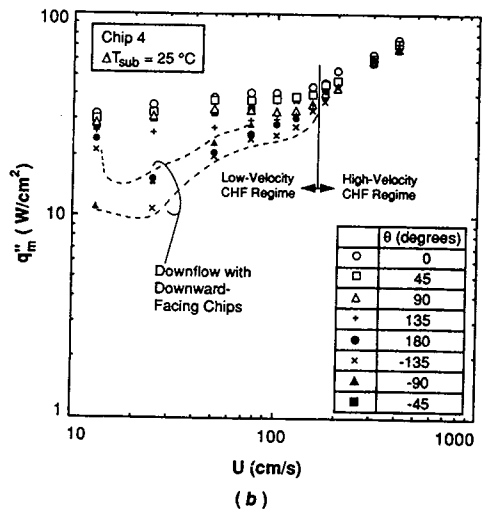

(b)

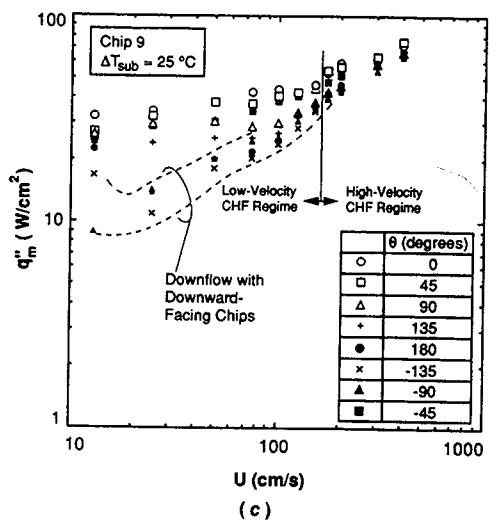

(c)

Fig. 7 Velocity effect on the critical heat flux for (*a*) Chip 1, (*b*) Chip 4, and (*c*) Chip 9 for an inlet subcooling of 25°C

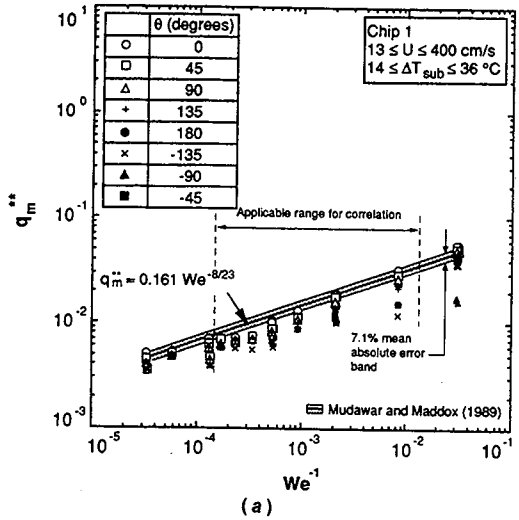

(a)

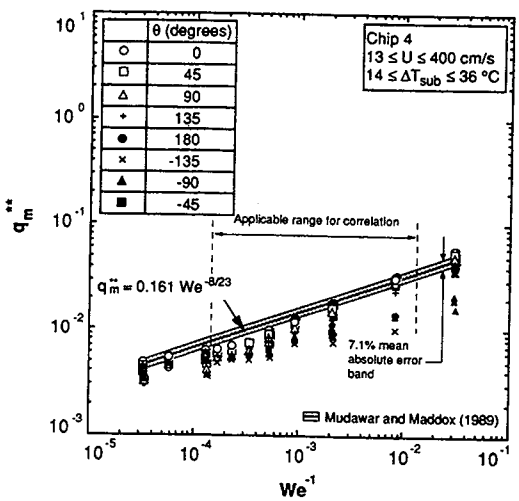

(b)

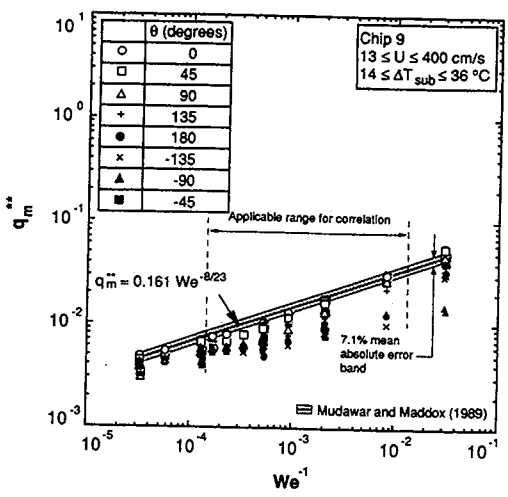

(c)

Fig. 8 Comparison of the nondimensional critical heat flux for (*a*) Chip 1, (*b*) Chip 4, and (*c*) Chip 9 with the Mudawar and Maddox (1989) correlation

at a lower inlet velocity for highly subcooled flow. Again, at these highly subcooled conditions, the effect of orientation on CHF became negligible for velocities greater than 150 cm/s.

The order in which the chips attained CHF was recorded. In general, the trends were similar to those reported by Willingham and Mudawar (1992b). That is, the most-upstream chips tended to reach CHF first during the near-saturated tests as the large degree of mixing and increased local fluid velocity caused by the void fraction appeared to enhance the heat transfer from the downstream chips. During the highly subcooled tests, the most-downstream chips tended to reach CHF first

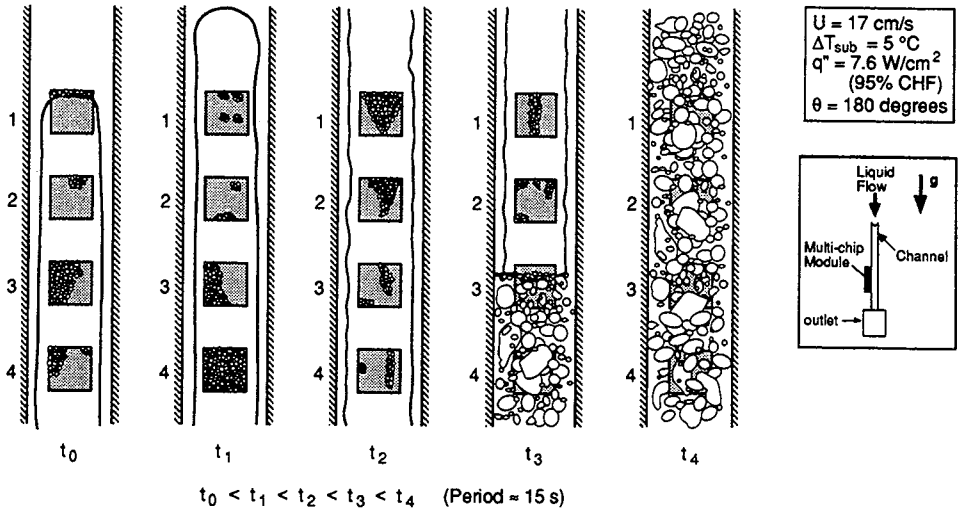

Fig. 9 Illustration of the periodic countercurrent formation of an elongated bubble

because of the streamwise warming of the fluid near the chips. There were some exceptions at low velocities as the test section was rotated from the upflow orientation. In the horizontal orientations ($\theta = \pm 90$ deg), the downstream chips reached CHF first during the near-saturated tests because of local liquid dryout. During the downflow tests at low velocities, both the upstream and the downstream chips tended to reach CHF first because of the vapor counterflow.

The relative spread in the CHF values for the nine chips during a particular experiment highlights the degree to which the presence of the multiple chips affected the individual CHF values. By defining a CHF bandwidth as the difference between the CHF values from the first and last chip to reach CHF (highest and lowest CHF values) divided by the average CHF value, Gersey and Mudawar (1992) found that CHF bandwidth was considerably less for upflow tests as compared to the corresponding downflow tests. For example, at $\Delta T_{sub} = 3°C$, upflow CHF bandwidth values ranged from 8.5 to 25.1 percent while the downflow values were between 12.8 and 49.2 percent. Critical heat flux bandwidth values were lower in the high-velocity CHF regime as compared to the low-velocity CHF regime. Increased liquid subcooling also served to decrease the CHF bandwidth.

Inlet subcooling was used to characterize the test conditions for all of the chips because no standard method exists for calculating a local streamwise subcooling along the multichip module. During the upflow tests, vapor did not spread out across the entire cross section of the channel, thus negating the usefulness of a mixing-cup temperature approximation. Although in downflow tests the vapor spread out across the channel, vapor stagnation and counterflow presented a further complication in calculating a local fluid temperature. The reader should consult the paper by Willingham and Mudawar (1992a) for analytical methods of calculating the streamwise increase in void faction.

Critical Heat Flux Limits

Critical Heat Flux Due to Local Dryout Caused by Intense Vapor Effusion. The ability to predict CHF is important to the design of a direct immersion electronic cooling system. To this end, several researchers have proposed empirical and semi-empirical equations in an effort to correlate CHF data. Figures 8(*a*), 8(*b*), and 8(*c*) compare the CHF values from Chips 1, 4, and 9 with the semi-empirical Mudawar and Maddox correlation (Mudawar and Maddox, 1989) for a single chip in subcooled upflow. Property data for FC-72 were obtained from the manufacturer (3M Company, 1986). Many of the upflow data fall within the error bounds of the correlation while the downflow data, especially at low velocities, are overpredicted by the correlation. Localized dryout was observed to be the cause of CHF for all of the upflow tests and the downflow tests at high velocities. These are the same tests that showed an insensitivity to orientation. This suggests that the Mudawar and Maddox correlation can be used to predict CHF for both upflow orientations and downflow orientations when the effect of orientation is negligible.

Critical Heat Flux Due to Stratification ($\theta \approx -90$ deg). As mentioned earlier, the vapor and liquid phases were observed to separate when the channel was oriented at $\theta = -90$ deg causing dryout on the surfaces of the downstream chips. The vapor and liquid also separated at $\theta = 90$ deg, but the liquid remained in contact with the surfaces of the chips because the chips were upward facing. Phase stratification was only observed at the lowest velocity tested, 13 cm/s, although the CHF values were still less than for the upflow conditions for velocities up to 150 to 200 cm/s. Because the vapor phase can possess a much larger velocity than the liquid when the phases are separated (Dukler and Taitel, 1986), the large velocity difference between the two phases could lead to interfacial waviness, density oscillations, and eventually to plug flow. This may actually aid in chip wetting at $\theta = -90$ deg but at the expense of undesirable flow instabilities.

Critical Heat Flux Due to Vapor Counterflow in Downflow ($\theta \approx 135$, -135, and 180 deg). At the lowest velocity, $U = 13$ cm/s, vapor bubbles coalesced into an elongated bubble, which moved counter to the liquid flow. This movement apparently increased the liquid contact with the chip surface because the CHF values when counterflow was present were higher than the tests at $U = 25$ cm/s where vapor stagnation occurred. As the inlet downflow velocity was reduced to zero, Mishima et al. (1985) and Mishima and Nishihara (1985) observed that flooding was responsible for CHF. The flow rates in the present study were large enough that flooding did not occur, but the large elongated bubbles that formed in the channel served to limit the replenishment of liquid to the chip surface in a manner similar to that of flooding. Figure 9 illustrates the development of an elongated bubble at $U = 17$ cm/s and $\theta = 180$ deg. In a periodic fashion, the elongated bubble formed and hovered over the chips before moving counter to the liquid flow. While the bubble moved up the channel, it condensed such that only a small amount of vapor was observed to enter the upstream reservoir of the test section. As the bubble condensed and decreased in size, its movement became erratic, at times flowing

cocurrent and countercurrent to the liquid. Also, a large degree of mixing occurred around the chips before the formation of the next elongated bubble. Boiling was observed at the leading edge of the elongated bubble at the upstream portion of Chip 1, and intense boiling was observed to take place sporadically on the chip surfaces highlighting the existence of a thin liquid film beneath the elongated bubble. Between the periods of intense boiling, the chip surfaces became momentarily dry. Critical heat flux occurred when the chip surfaces remained dry for a prolonged duration.

Critical Heat Flux Due to Bubble Stagnation ($\theta \approx 135, -135,$ and 180 deg). During the low inlet velocity experiments at orientations of 135, 180 and -135 deg, vapor bubbles stagnated in the channel. At $\theta = -135$ and 180 deg, where the chips were downward facing, the stagnant bubbles starved the chips of liquid causing a large decrease in CHF compared to the 0-deg reference as shown in Figs. 6(*a*)–6(*c*) and 7(*a*)–7(*c*). However, at $\theta = 135$ deg where the chips were upward facing, the stagnant bubbles accumulated on the Lexan window permitting liquid to continually contact the chip surfaces; CHF values for this orientation were lower than for the 0-deg reference but not by as much as the downward-facing chips. Additional experiments were performed at $\theta = 180$ deg with near-saturated flow to determine the range of inlet velocities where bubble stagnation occurs. Flow visualization revealed that, for $U = 13$ to 31 cm/s, vapor tended to collect over the chips and form an elongated bubble typical of slug flow. Below $U = 25$ cm/s, the elongated bubbles occasionally moved in the channel counter to the liquid motion and eventually condensed inside the channel. For velocities above 25 cm/s, the elongated bubbles were observed to move in the same direction as the fluid and exit the channel. Very little bubble movement was observed at $U \approx 25$ cm/s, and as a result, CHF was lowest at this velocity with the 135, 180 and -135 deg orientations.

Since vapor stagnation has been shown to decrease CHF, predicting the downflow velocity at which bubble stagnation occurs is of vital importance. By equating the buoyancy force and the drag force on the bubble, an initial estimate of the stagnation velocity can be made. Because of its simplicity, the stagnation velocity (terminal velocity) for spherical and elongated bubbles in quiescent liquid has been extensively studied in infinite media (Haramathy, 1960; Wallis, 1974; Ishii and Zuber, 1979), and in a confining system of circular tubes and rectangular channels (Uno and Kintner, 1956; Harmathy, 1960; Davidson and Harrison, 1963; Collins, 1965; Wallis, 1969). Most of the previously derived correlations require knowledge of the bubble size in order to calculate a hydraulic bubble diameter, thus some estimate of vapor volume would be needed in order to utilize the correlations successfully.

When the volume of vapor in the bubble is increased, the bubble either grows in size or breaks into smaller bubbles, depending upon the ability of surface tension to resist interfacial instabilities. When flow boundaries restrict the bubble, the bubble may grow into an elongated bubble typical of slug flow such as the bubbles observed in the present study. The thin film-like flow around the elongated bubble produces a different stagnation velocity than that for a spherical or cap bubble. Many researchers have studied the stagnation velocity tests with elongated bubbles moving in vertical tubes and rectangular channels with no net liquid flow (Dumitrescu, 1943; Davies and Taylor, 1950; Haramathy, 1960; White and Beardmore, 1962; Brown, 1965; Zukoski, 1966; Stewart and Davidson, 1967). From their correlations, it is evident that the stagnation velocity is a function of the channel hydraulic diameter and liquid properties. For the most part, the analytic and empirical correlations agreed with each other. Most of the correlations predict a stagnation velocity (terminal velocity) of about 10 cm/s for FC-72 rising in quiescent fluid. Zukoski (1966) also tested orientations other than vertical and found that a maximum bubble rise velocity in quiescent liquid exists near the 45-deg orientation. Zukoski also had success in collapsing terminal velocity data for air in both acetone and water using a surface tension parameter, $4\sigma/(\rho_f - \rho_g)gD_h^2$.

The bubble velocity is also affected by the liquid velocity when a net liquid flow exists in the system, increasing when the liquid flow opposes gravity (upflow) and decreasing when the liquid flows with gravity (downflow). In upflow, the bubble velocity was found to be a function of the superficial liquid and vapor velocities and the terminal bubble velocity (Griffith and Wallis, 1961; Nicklin et al., 1962; Zuber and Findlay, 1965). This suggests that, in the absence of very high void fractions (total liquid dryout), upflow enhances vapor exit from the system, thus benefiting heat transfer. Although Griffith and Wallis (1961) did not correlate their downflow data, they observed that, for some downflow velocities, the shape and upward velocity of the vapor bubbles were erratic. Nicklin et al. (1962) recorded data with liquid downflow; however, the large degree of data scatter precluded their ability to correlate the data. They reported that elongated bubbles stagnated in their system at approximately 15 cm/s. Mishima and Nishihara (1985) observed bubble stagnation over an inlet mass velocity range of 150 to 200 kg/m^{2}s which, for water, amounts to a stagnation velocity of approximately 15 to 20 cm/s. Mishima and Nishihara proposed an empirical correlation based on the drift flux model for the stagnation velocity in downflow. Their method predicts a stagnation velocity of 9.15 cm/s for the present study. Bubble stagnation was also reported at a downflow inlet velocity of 26 cm/s during the boiling of water in a centrally heated annular system (Bibeau and Salcudean, 1990). Although the stagnation velocity was not investigated, Bartolini et al. (1983) observed a much higher void fraction of water vapor in the annulus at a downflow velocity of 20 cm/s. Because of the differences in thermophysical properties between fluids, a direct comparison of the stagnation velocities between experiments may not be accurate, rather some type of nondimensionalization, like that of Zukoski's (1966), may need to be employed.

Nevertheless, the previous studies illustrate that relative vapor movement, particularly stagnation, occurs at low downflow velocities. It is apparent that all the previous studies seem to point to a critical downflow velocity range between 10 and 30 cm/s, where stagnation most likely will occur and should be avoided. This range agrees well with the observed stagnation inlet velocity range of 13–31 cm/s. Downflow velocities below stagnation also pose flow stability problems even though CHF may actually increase. The erratic, up and down movement of the elongated bubble in the present study highlights the presence of undesirable, albeit small, flow oscillations. At extremely small inlet velocities, CHF could potentially become lower and unpredictable when this flow oscillations is coupled with the large void fraction in the vicinity of the heat sources. These flow oscillations could also pose problems in a multichannel (e.g., parallel flow into several modules) where pressure and density waves could momentarily redistribute the flow into the parallel channels, thereby decreasing the inlet liquid flow rate. In light of the unpredicatable nature of vapor movement at low downflow velocities, sufficiently large velocities should be utilized to ensure cocurrent vapor flow.

Critical Heat Flux Envelope. A polar representation of the four CHF regimes is shown in Fig. 10 for an inlet subcooling of 3°C; however, similar trends were observed for highly subcooled flow. The figure is meant as an illustration and does not suggest that the boundaries between CHF regimes are well defined and absolute. Stratification occurred at low velocities for angles near $\theta = -90$ deg while vapor counterflow was responsible for CHF for the rest of the downflow orientations. If lower downflow velocities were tested, perhaps flooding would have been observed to initiate CHF. For slightly higher

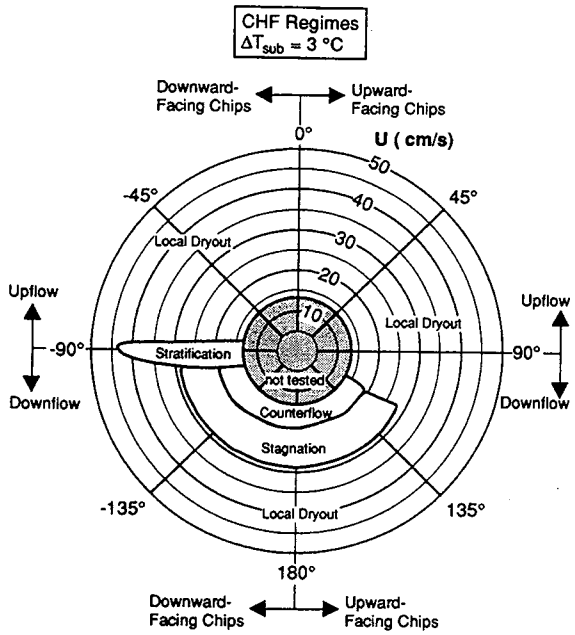

Fig. 10 Polar representation of the critical heat flux regimes at an inlet subcooling of 3°C

velocities, CHF was a result of vapor stagnation. Critical heat flux for the rest of the downflow experiments and all of the upflow experiments was caused by localized dryout of the chip surface.

In order to compare the CHF results of the present study with previous studies, the minimum CHF data at $\theta = 0$, 135, 180, and -135 deg are shown in Figs. 11(*a*) and 11(*b*) for inlet subcoolings of 3 and 25°C, respectively, using the nondimensional parameters suggested by Mishima and Ishii (1982) and Mishima and Nishihara (1985). Although the data for $\theta = \pm 135$ deg do not correspond to vertical downflow, they are included because visual observations suggest that the hydrodynamic and thermal mechanisms in the channel are similar to those at $\theta = 180$ deg. The CHF correlations listed in Table 2 are included in Figs. 11(*a*) and 11(*b*) for comparison with the data. Table 2 includes correlations for the following:

1 Pool boiling: reference
2 Flooding: limiting condition
3 $x_e = 0$ and $x_e = 1$: net vapor generation and liquid dryout, respectively
4 Transition from churn turbulent to annular flow
5 H-regime, HP-regime (Katto, 1981), and small L_{he}/D_{he} ratio (Katto and Kurata, 1980) correlations: CHF envelope for long, continuous heaters
6 Mudawar and Maddox (1989): localized dryout of the chip surface

As shown in Fig. 11(*a*) for near-saturated flow, the CHF values for the 0-deg reference were for the most part above the flooding and pool boiling limits while the downflow values were predominantly below both limits. This illustrates that the stratification, vapor counterflow, and vapor stagnation regimes can cause a lower CHF than for flooding. Forced-convection CHF can be lower than pool boiling CHF because the liquid flow confines the vapor near the chip surface, thus inhibiting liquid replenishment. Even though most of the CHF data fell below the $x_e = 0$ line, a large void fraction was observed in the channel for the near-saturated tests; thus, the flow was far from thermal equilibrium. Perhaps boiling on small discrete heat sources does not provide the same degree of mixing as experiments with a continuous heated wall because of vapor condensation between the heat sources. As a result, local void fractions at the heater were higher than the equilibrium assumptions would predict.

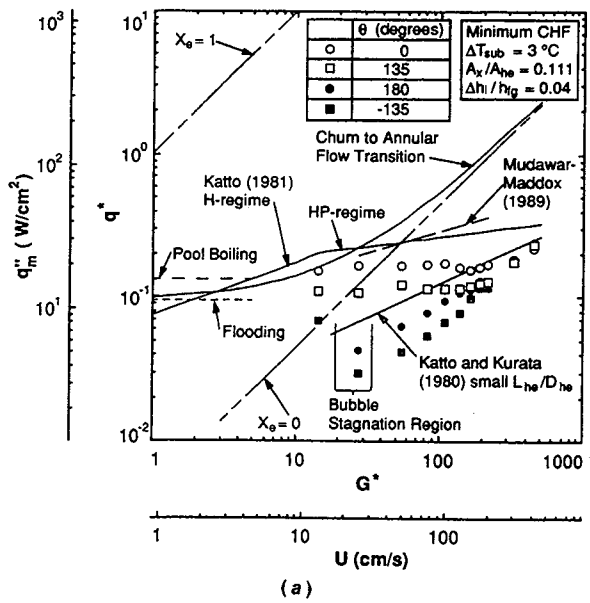

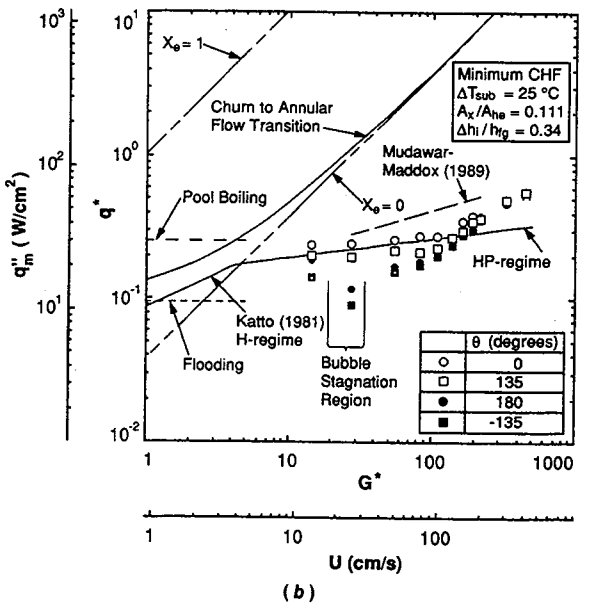

Fig. 11 Comparison of the minimum critical heat flux with previous correlations for inlet subcoolings of (*a*) 3°C and (*b*) 25°C

The Mudawar and Maddox correlation (Mudawar and Maddox, 1989) sets the upper heat flux limit of CHF associated with local dryout of the chip surface, and the minimum CHF data are overpredicted by the correlation. As shown in Figs. 8(*a*), 8(*b*), and 8(*c*), CHF for many of the chips was successfully predicted by the Mudawar and Maddox correlation. These values were, in many cases, larger than the minimum CHF, which did not necessarily occur at the same chip for all of the conditions. The empirical correlations of Katto (1981) were developed for rectangular channels continuously heated from one or two sides also appear to form an upper limit. Katto and Kurata (1980) proposed that their empirical CHF correlation for saturated parallel jet flow on a submerged heater could also be utilized in a heated annulus and other systems with small L_{he}/D_{he} ratios. As shown in Fig. 11(*a*), the correlation intersects the data at high velocities, but fails to predict either the upflow or downflow data at low velocities.

Figure 11(*b*) shows almost all of the highly subcooled data are above the flooding limit. Although vapor stratification,

Table 2 Correlations for Fig. 11

Reference	Correlation	Equation	Notes
Wallis (1969)	Flooding	$q''_F = C^2 \frac{A_x}{A_{he}} \left(\frac{D_h^2 g (\rho_f - \rho_g)}{\sigma}\right)^{1/4} \left[1 + \left(\frac{\rho_g}{\rho_f}\right)^{1/4}\right]^{-2}$	$C = 0.725$ Wallis (1969) $C = 0.6\left(\frac{L_{he}}{D_h}\right)^{0.05}$ for fluids with different ρ_g/ρ_f ratios (Nejat, 1981)
Zuber et al. (1961)	Pool Boiling	$q''_{pb} = 0.131 \left(\frac{\rho_f + \rho_g}{\rho_f}\right)^{1/2} \left(1 + 5.3 \frac{\sqrt{k_f \rho_f c_{pf}}}{\rho_g h_{fg}} \left(\frac{g \sigma (\rho_f - \rho_g)}{\rho_g^2}\right)^{1/8} \left(\frac{g (\rho_f - \rho_g)}{\sigma}\right)^{1/4} \Delta T_{sub}\right)$	Derived for an infinite horizontal plate
	$x_e = 0.0$	$q''_{x0} = \frac{A_x}{A_{he}} \frac{\Delta h_i}{h_{fg}} G''$	Energy balance
	$x_e = 1.0$	$q''_{x1} = \frac{A_x}{A_{he}} \left(1 + \frac{\Delta h_i}{h_{fg}}\right) G''$	Energy balance
Mishima and Ishii (1982)	Churn Turbulent to Annular Flow Transition	$q''_{ca} = q''_F + q''_{x0}$	Also observed by Mishima and Nishihara (1985)
Katto (1981)	H-Regime	$q''_H = \frac{0.15}{1 + 0.0077 \frac{L_{he}}{D_{he}}} \left(\frac{\rho_g}{\rho_f}\right)^{0.133} \left(1 + k \frac{\Delta h_i}{h_{fg}}\right) \left(\frac{\rho_f \lambda}{L_{he} \rho_g}\right)^{1/3} (G'')^{1/3}$, where $k = \frac{5}{9}\left(0.0308 + \frac{D_{he}}{L_{he}}\right) \left(\frac{\rho_g}{\rho_f}\right)^{-0.133} \left(\frac{\rho_f \lambda}{L_{he} \rho_g}\right)^{-1/3} (G'')^{2/3}$	Made for water in a rectangular channel heated on one or two sides for $20 \le L_{he}/D_{he} \le 500$
	HP-Regime	$q''_{HP} = \frac{0.26}{1 + 0.0077 \frac{L_{he}}{D_{he}}} \left(\frac{\rho_g}{\rho_f}\right)^{0.133} \left(\frac{\rho_f \lambda}{L_{he} \rho_g}\right)^{0.433} \left(\frac{L_{he}}{D_{he}}\right)^{0.171} (G'')^{0.134}$	
Katto and Kurata (1980)		$q''_K = 0.186 \left(\frac{\rho_g}{\rho_f}\right)^{0.559} \left(\frac{\rho_f \lambda}{L_{he} \rho_g}\right)^{0.264} (G'')^{0.472}$	Correlates saturated water and R-113 data for parallel jet of water over a submersed heater Shown to work for annuli with small L_{he}/D_{he} ratios
Mudawar and Maddox (1989)	Local Dryout	$q''_{MM} = 0.161\, G''\, We^{-8/23} \left(\frac{\rho_f}{\rho_g}\right)^{-8/23} \left(\frac{L}{D_h}\right)^{1/23} \left(1 + \frac{c_{pf} \Delta T_{sub}}{h_{fg}}\right)^{7/23} \left(1 + 0.021 \frac{\rho_f c_{pf} \Delta T_{sub}}{\rho_g h_{fg}}\right)^{16/23}$	Developed for an isolated heat source in a rectangular channel with FC-72

counterflow, and stagnation caused a substantial decrease in CHF for the downflow tests, the CHF values associated with these regimes were not below the flooding value like the corresponding near-saturated tests. Some of the 0-deg data and all of the low-velocity downflow data are below the pool boiling limit. Figure 11(*b*) shows that the Mudawar and Maddox correlation is once again an upper limit for CHF. The correlations of Katto (1981) intersect the low velocity upflow data but fail to predict the rest of the data.

Conclusions

The effect of flow orientation on CHF of FC-72 from a linear array of nine, in-line simulated microelectronic chips was investigated. The following conclusions are drawn:

1 Orientation had a negligible effect on CHF for inlet fluid velocities greater than 200 cm/s for near-saturated flow and 150 cm/s for highly subcooled flow. Below these velocities, upflow orientations yielded higher CHF values as compared to downflow and horizontal flow with downward-facing chips.

2 Critical heat flux was the result of localized dryout on the chip surface for the upflow tests and the downflow tests with relatively high flow rates. During the low-velocity tests, CHF values were smaller for downflow and horizontal, downward-facing chip tests because of liquid blockage by vapor counterflow, vapor stagnation, and stratification in the channel.

3 Critical heat flux values measured for downward-facing chips subjected to downflow ($\theta = 180$ and -135 deg) and downward-facing chips with horizontal flow ($\theta = -90$ deg) were as low as 18 percent of their respective vertical upflow values.

4 The inlet liquid velocity that caused the vapor to stagnate in the channel was measured to be around 25 cm/s at $\theta = 180$ deg. The measured stagnation velocity agreed with previous studies, which found the stagnation velocity to be a function of the bubble terminal rise velocity in quiescent liquid and the velocity of incoming liquid. Because of the considerable effect of downflow on CHF, it is recommended that forced-convection cooling systems avoid downflow or use a sufficiently large inlet liquid velocity to overcome the orientation effects.

5 In comparing the present data to previously derived CHF correlations, CHF values for near-saturated downflow were found smaller than the heat fluxes corresponding to pool boiling and flooding-induced CHF. Critical heat fluxes for highly subcooled flow were all greater than the flooding value, but, again, many of the low velocity tests were below pool boiling. The Mudawar and Maddox (1989) correlation for local dryout on an isolated chip in vertical upflow provided an upper limit for the measured CHF values.

Acknowledgments

Support of this work by a grant from the Industrial Chemical Products Division of 3M is gratefully acknowledged.

References

3M Company, 1986, "Product Manual: Fluorinert Electronic Liquids," Industrial Chemical Products Division, 3M Center, St. Paul, MN.

Bartolini, R., Gugliemini, G., and Nannei, E., 1983, "Experimental Study on Nucleate Boiling of Water in Vertical Upflow and Downflow," *International Journal of Multiphase Flow*, Vol. 9, pp. 161–165.

Bibeau, E. L., and Salcudean, M., 1990, "The Effect of Flow Direction on Void Growth at Low Velocities and Low Pressure," *International Communications in Heat and Mass Transfer*, Vol. 17, pp. 19–25.

Brown, R. A. S., 1965, "The Mechanics of Large Gas Bubbles in Tubes: I. Bubble Velocities in Stagnant Liquids," *The Canadian Journal of Chemical Engineering*, Vol. 43, pp. 217–223.

Chen, L. T., 1978, "Heat Transfer to Pool-Boiling Freon From Inclined Heating Plate," *Letters in Heat and Mass Transfer*, Vol. 5, pp. 111–120.

Class, C. R., DeHaan, J. R., Piccone, M., and Cost, R. B., 1960, "Boiling Heat Transfer to Liquid Hydrogen From Flat Surfaces," *Advances in Cryogenic Engineering*, K. D. Timmerhaus, ed., Vol. 5, Plenum Press, New York, pp. 254–261.

Collins, R., 1965, "A Simple Model of the Plane Gas Bubble in a Finite Liquid," *Journal of Fluid Mechanics*, Vol. 22, pp. 763–771.

Danielson, R. D., Tousignant, L., and Bar-Cohen, A., 1987, "Saturated Pool Boiling Characteristics of Commercially Available Perfluorinated Inert Liquids," *Proceedings of the 1987 ASME/JSME Thermal Engineering Joint Conference*, P. J. Marto and I. Tanasawa, ed., Vol. 3, Honolulu, HI, pp. 419–430.

Davidson, J. F., and Harrison, D., 1963, *Fluidised Particles*, Cambridge University Press, Cambridge, United Kingdom.

Davies, R. M., and Taylor, G. I., 1950, "The Mechanics of Large Bubbles

Rising Through Extended Liquids and Through Liquids in Tubes," *Proceedings of the Royal Society of London Series A*, Vol. 200, pp. 375-390.

Dukler, A. E., and Taitel, Y., 1986, "Flow Pattern Transitions in Gas-Liquid Systems: Measurement and Modeling," *Multiphase Science and Technology*, G. F. Hewitt, J. M. Delhaye, and N. Zuber, ed., Vol. 2, Hemisphere Publishing Corp., New York, pp. 1-94.

Dumitrescu, D. T., 1943, "Stromung an einer Luftblase im senkrechten Rohr," *Zeitschrift für Angewandte Mathematik und Mechanik*, Vol. 23, pp. 139-149.

Gambill, W. R., 1968, "Burnout in Boiling Heat Transfer—Part II: Subcooled Forced-Convection Systems," *Nuclear Safety*, Vol. 9, pp. 467-480.

Gersey, C. O., and Mudawar, I., 1992, "Effects of Orientation on Critical Heat Flux From Chip Arrays During Flow Boiling," ASME *Journal of Electronic Packaging*, Vol. 114, pp. 290-299.

Githinji, P. M., and Sabersky, R. H., 1963, "Some Effects of the Orientation of the Heating Surface in Nucleate Boiling," ASME JOURNAL OF HEAT TRANSFER, Vol. 85, p. 379.

Griffith, P., and Wallis, G. B., 1961, "Two-Phase Slug Flow," ASME JOURNAL OF HEAT TRANSFER, Vol. 83, pp. 307-320.

Haramathy, T. Z., 1960, "Velocity of Large Drops and Bubbles in Media of Infinite or Restricted Extent," *AIChE Journal*, Vol. 6, pp. 281-288.

Ishii, M., and Zuber, N., 1979, "Drag Coefficient and Relative Velocity in Bubbly, Droplet, or Particulate Flows," *AIChE Journal*, Vol. 25, pp. 843-855.

Katto, Y., and Kurata, C., 1980, "Critical Heat Flux of Saturated Convective Boiling on Uniformly Heated Plates in a Parallel Flow," *International Journal of Multiphase Flow*, Vol. 6, pp. 575-582.

Katto, Y., 1981, "General Features of CHF of Forced Convection Boiling in Uniformly Heated Rectangular Channels," *International Journal of Heat and Mass Transfer*, Vol. 24, pp. 1413-1419.

Kumar, V., Prasad, M., Verma, M. K., and Garg, N. S., 1990, "Effect of Inclination on Pool Boiling Heat Transfer From a Flat Plate," *Indian Chemical Engineer*, Vol. 32, pp. 61-64.

Lee, T. Y., and Simon, T. W., 1989, "Critical Heat Flux in Forced Convection Boiling From Small Regions," *Heat Transfer in High Energy/High Heat Flux Applications*, R. J. Goldstein, L. C. Chow, and E. E. Anderson, eds., ASME HTD-Vol. 119, pp. 1-7.

Maddox, D. E., and Mudawar, I., 1989, "Single and Two-Phase Convective Heat Transfer From Smooth and Enhanced Microelectronic Heat Sources in a Rectangular Channel," ASME JOURNAL OF HEAT TRANSFER, Vol. 111, pp. 1045-1052.

Marcus, B. D., and Dropkin, D., 1963, "The Effect of Surface Configuration on Nucleate Boiling Heat Transfer," *International Journal of Heat and Mass Transfer*, Vol. 6, pp. 863-867.

McGillis, W. R., Carey, V. P., and Strom, B. D., 1991, "Geometry Effects on Critical Heat Flux for Subcooled Convective Boiling From an Array of Heated Elements," ASME JOURNAL OF HEAT TRANSFER, Vol. 113, pp. 463-471.

Mishima, K., and Ishii, M., 1982, "Critical Heat Flux Experiments Under Low Flow Conditions in a Vertical Annulus," ANL 82-6, Argonne National Laboratory Report.

Mishima, K., and Nishihara, H., 1985, "The Effect of Flow Direction and Magnitude on CHF for Low Pressure Water in Thin Rectangular Channels," *Nuclear Engineering and Design*, Vol. 86, pp. 165-181.

Mishima, K., Nishihara, H., and Michiyoshi, I., 1985, "Boiling Burnout and Flow Instabilities for Water Flowing in a Round Tube Under Atmospheric Pressure," *International Journal of Heat and Mass Transfer*, Vol. 28, pp. 1115-1129.

Moffat, R. J., 1988, "Describing the Uncertainties in Experimental Results," *Experimental Thermal and Fluid Science*, Vol. 1, pp. 3-17.

Mudawar, I., and Anderson, T. M., 1989a, "High Flux Electronic Cooling by Means of Pool Boiling—Part 1: Parametric Investigation of the Effects of Coolant Variation, Pressurization, Subcooling, and Surface Augmentation," *Heat Transfer in Electronics 1989*, R. K. Shah, ed., ASME HTD-Vol. 111, pp. 25-34.

Mudawar, I., and Anderson, T. M., 1989b, "High Flux Electronic Cooling by Means of Pool Boiling—Part 2: Optimization of Enhanced Surface Geometry," *Heat Transfer in Electronics 1989*, R. K. Shah, ed., ASME HTD-Vol. 111, pp. 35-49.

Mudawar, I., and Maddox, D. E., 1989, "Critical Heat Flux in Subcooled Flow Boiling of Fluorocarbon Liquid on a Simulated Electronic Chip in a Vertical Rectangular Channel," *International Journal of Heat and Mass Transfer*, Vol. 32, pp. 379-394.

Mudawar, I., and Maddox, D. E., 1990, "Enhancement of Critical Heat Flux From High Power Microelectronic Heat Sources in a Flow Channel," ASME *Journal of Electronic Packaging*, Vol. 112, pp. 241-248.

Nakayama, W., Nakjima, T., and Hirasawa, S., 1984, "Heat Sink Studs Having Enhanced Boiling Surfaces for Cooling of Microelectronic Components," ASME Paper No. 84-WA/HT-89.

Nejat, Z., 1981, "Effect of Density Ratio on Critical Heat Flux in Closed End Vertical Tubes," *International Journal of Multiphase Flow*, Vol. 7, pp. 321-327.

Nicklin, D. J., Wilkes, J. O., and Davidson, J. F., 1962, "Two-Phase Flow in Vertical Tubes," *Transactions of the Institution of Chemical Engineers*, Vol. 40, pp. 61-68.

Nishikawa, K., Fujita, Y., Uchida, S., and Ohta, H., 1983, "Effect of Heating Surface Orientation on Nucleate Boiling Heat Transfer," *Proceedings of the ASME-JSME Thermal Engineering Joint Conference 1983*, Y. Mori and W. J. Yang, eds., Vol. 1, Honolulu, HI, pp. 129-136.

Park, K. A., and Bergles, A. E., 1988, "Effects of Size of Simulated Microelectronic Chips on Boiling and Critical Heat Flux," ASME JOURNAL OF HEAT TRANSFER, Vol. 110, pp. 728-734.

Park, K. A., Bergles, A. E., and Danielson, R. D., 1990, "Boiling Heat Transfer Characteristics of Simulated Microelectronic Chips With Fluorinert Liquids," *Heat Transfer in Electronic and Microelectronic Equipment*, A. E. Bergles, ed., Hemisphere Publishing Corp., New York, pp. 573-588.

Samant, K. R., and Simon, T. W., 1989, "Heat Transfer From a Small Heated Region to R-113 and FC-72," ASME JOURNAL OF HEAT TRANSFER, Vol. 111, pp. 1053-1059.

Simoneau, R. J., and Simon, F. F., 1966, "A Visual Study of Velocity and Buoyancy Effects on Boiling Nitrogen," NASA, TN D-3354.

Stewart, P. S. B., and Davidson, J. F., 1967, "Slug Flow in Fluidised Beds," *Powder Technology*, Vol. 1, pp. 61-80.

Uno, S., and Kintner, R. C., 1956, "Effect of Wall Proximity on the Rate of Rise of Single Air Bubbles in a Quiescent Liquid," *AIChE Journal*, Vol. 2, pp. 420-425.

Wallis, G. B., 1969, *One-Dimensional Two-Phase Flow*, McGraw-Hill, New York.

Wallis, G. B., 1974, "The Terminal Speed of Single Drops or Bubbles in an Infinite Medium," *International Journal of Multiphase Flow*, Vol. 1, pp. 491-511.

White, E. T., and Beardmore, R. H., 1962, "The Velocity of Rise of Single Cylindrical Air Bubbles Through Liquids Contained in Vertical Tubes," *Chemical Engineering Science*, Vol. 17, pp. 351-361.

Willingham, T. C., Gersey, C. O., and Mudawar, I., 1991, "Forced Convective Boiling From an Array of In-Line Heat Sources in a Flow Channel," *Proceedings of the ASME-JSME Thermal Engineering Joint Conference 1991*, J. R. Lloyd and Y. Kurosaki, eds., Vol. 2, Reno, NV, pp. 365-374.

Willingham, T. C., and Mudawar, I., 1992a, "Channel Height Effects on Forced-Convection Boiling and Critical Heat Flux From a Linear Array of Discrete Heat Sources," *International Journal of Heat and Mass Transfer*, Vol. 35, pp. 1865-1880.

Willingham, T. C., and Mudawar, I., 1992b, "Forced-Convection Boiling and Critical Heat Flux From a Linear Array of Discrete Heat Sources," *International Journal of Heat and Mass Transfer*, Vol. 35, pp. 2879-2890.

Zuber, N., and Findlay, J. A., 1965, "Average Volumetric Concentration in Two-Phase Flow Systems," ASME JOURNAL OF HEAT TRANSFER, Vol. 87, pp. 453-468.

Zuber, N., Tribus, M., and Westwater, J. W., 1961, "The Hydrodynamic Crisis in Pool Boiling of Saturated and Subcooled Liquids," *International Developments in Heat Transfer: Proceedings of the 1961-62 International Heat Transfer Conference*, Boulder, CO, pp. 230-236.

Zukoski, E. E., 1966, "Influence of Viscosity, Surface Tension, and Inclination Angle on Motion of Long Bubbles in Closed Tubes," *Journal of Fluid Mechanics*, Vol. 25, pp. 821-837.